Author's personal copy

Materials and Design 32 (2011) 192–197

Contents lists available at ScienceDirect

Materials and Design

journal homepage: www.elsevier.com/locate/matdes

Contribution of Ti addition to characteristics of extruded Cu40Zn brass alloy prepared by powder metallurgy

Shufeng Li *, Hisashi Imai, Haruhiko Atsumi, Katsuyoshi Kondoh

Department of Composites Processing, Joining and Welding Research Institute, Osaka University, 567-0047 11-1, Mihogaoka, Ibaraki, Osaka, Japan

ARTICLE INFO

Article history:
Received 15 February 2010
Accepted 7 June 2010
Available online 10 June 2010

Keywords:
Brass
Spark plasma sintering
Precipitation hardening

ABSTRACT

The aim of this paper was to investigate the properties of Cu40ZnTi for the purpose of developing a new high-strength, lead-free brass by powder metallurgy. The effect of Ti addition on precipitation hardening behavior of Cu40Zn (denoted as BS40) brass was studied with respect to mechanical properties and microstructures. BS40 and Cu40Zn – 1.0 wt.%Ti (denoted as BS40-A) brass powders were prepared by water atomization process, and β phase was retained in the raw powders predominately. The BS40 powder and Ti powder were elementally mixed to prepare Cu40Zn + 0.5 wt.%Ti (denoted as BS40-B) and Cu40Zn + 1.0 wt.%Ti (denoted as BS40-C) premixed powders. The alloy powders and premixed powders were solidified at 1053 K for 600 s by spark plasma sintering (SPS) and extruded subsequently. It was observed that Cu_2ZnTi intermetallic compound (IMC) and CuZnTi metastable phase resulted from the reaction between Ti and CuZn showed distinct grain refinement effect on extruded Cu40Zn brass. Thus, the excellent strengthening effect processes by precipitation hardening and deform working was obtained, which responding to an yield strength of 345 MPa, and a ultimate tensile strength of 597 MPa, showed 65.9% and 30.4% higher than that of extruded Cu40Zn brass, respectively.

Crown Copyright © 2010 Published by Elsevier Ltd. All rights reserved.

1. Introduction

Brasses are widely used in many applications, such as lead frames, connectors and other electronic components, pipes, valves, and fittings in potable water system and so on, because of their excellent electrical and thermal conductivities, outstanding resistance to corrosion, ease of fabrication, and good strength and fatigue resistance [1]. In recent years, the development of high-strength and high-conductive brasses are urgent to satisfy the new demands of the electronic industry, automotive and aerospace applications, household appliances, etc. [2]. On the other hand, the stricter regulations for allowable lead content levels in products provide the impetus for the development of lead-free brass [3–5]. These applications require alloys with unique combinations of strength and conductivity coupled with environment amiability.

Precipitation hardening is the primary method of developing high-strength copper-based alloys, because it could effectively improve the mechanical properties of alloys. The binary phase diagrams of copper alloys [6] indicate that Cr, Fe, Ti, Co, Mg, Sn, etc. could be served as candidate alloying elements for precipitation strengthening, to develop high-strength and high-conductivity copper alloys, because of the solid solubility of these alloying elements in copper would decrease sharply with the decreasing temperature.

Cu–Ti binary alloys are precipitation strengthened by spinodal decomposition mechanism [7,8] involving composition modulations and long range ordering in the initial stages of ageing. The tensile strength value of 930 N/mm^2 was obtained for Cu–5.4 wt.%Ti alloy by the precipitation of a coherent and metastable fine precipitation of Cu_4Ti (β′) [9]. According to Kumar et al. [10], the phase diagram shows five intermediate phases in the Cu–Ti system, i.e. Cu_4Ti, Cu_3Ti_2, Cu_4Ti_3, CuTi and $CuTi_2$, which indicates Ti is an attractive candidate to develop high strength copper alloys by precipitation hardening. However, few literatures available reported the influence of Ti addition on mechanical properties of Cu40Zn brass, which is worth to be investigating. The research is a part of a project whose scope was to investigate the engineering properties of new commercial alloy formulations base on the Cu40Zn duplex phase brass. The primary purpose of this paper is to explore the possibility that new high strength lead-free brass could be developed by novel spark plasma sintering (SPS), employing water atomized powders as raw materials. The properties of precipitation hardening response of Ti were employed and the mechanical properties and microstructure were investigated in detail.

2. Experimental

As-received water atomized BS40 and BS40-A alloy powders (Nihon atomized metal powders Co.) were used as raw materials. The compositions of the raw powder were shown in Table 1. To

* Corresponding author. Tel.: +81 080 5513 6888; fax: +81 06 6879 8669.
E-mail address: shufengli@hotmail.com (S. Li).

0261-3069/$ - see front matter Crown Copyright © 2010 Published by Elsevier Ltd. All rights reserved.
doi:10.1016/j.matdes.2010.06.008

Author's personal copy

Table 1
Particle size and chemical compositions of the BS40 and BS40-A alloy powders.

Powders	Particle size (μm)		Mass%			
	Median size	Mean size	Zn	Ti	O	Cu
BS40	248	279	40	–	0.05	Bal.
BS40-A	106	150	41.19	0.99	0.23	Bal.

understand the effects of Ti contents on properties of brass, the powder of BS40-B and BS40-C were also prepared, respectively, by premixing BS40 powder and Ti powder for 2 h using a ball milling machine. For sintering, 300 g powder was loaded into a cylindrical graphite die and sintered using a DR.Sinter/SPS-1030 system (Sumitomo Coal Mining, Japan). The sintering temperature and pressure were set as 1053 K and 40 MPa. After holding at desired temperature for 600 s, the power was turned off and the sample was cooled in the chamber to less than 423 K. The sintering parameters were optimized to obtain a full density sample, and to avoid zinc vaporization at higher temperature, referring to the optimal sintering parameters for Cu40Zn brass at present experimental conditions in previous investigations [11].

The billets obtained with a diameter 42 mm were extruded with a load of 2000 kN by the hydraulic press machine (SHP-200-50, Shibayama Machine Co.). Before extrusion, the billets were preheated at 928 K for 30 min in nitrogen gas atmosphere, to ensure the billet having sufficient plastic deformation properties at present extrusion conditions. The final diameter after extrusion was of 7 mm, and the extrusion ratio was 37:1. The schematic sketch of the experimental procedure used to preparing samples is shown in Fig. 1. The extruded round bar were machined into test samples with 3 mm diameter in accordance with ICS 59.100.01. Tensile strength was conducted on a universal testing machine (Autograph AG-X 50 N, Shimadzu) with a strain rate of $5 \times 10^{-4}\,s^{-1}$. The strain was recorded by a CCD camera accessorized to the machine. Three samples at the same conditions were prepared for the tensile strength test in order to obtain the average value.

The phase compositions in samples were identified by using X-ray diffraction (Labx, XRD-6100, Shimadzu) referenced to the standard ICDD PDF cards available in the system software. In addition, the microstructure evolution of the raw powder and samples with the transversal and longitudinal cross-section to the extrusion direction, including fracture surface were conducted by using field-emission scanning electronic microscope (FE-SEM, JEM-6500F, JEOL), phases were examined by the energy-dispersive X-ray spectrometer (DES) equipped by the SEM.

3. Results and discussion

3.1. Characteristic of the as-received powders

The FE-SEM micrographs of the raw powders are depicted in Fig. 2. The BS40 and BS40-A particles show irregular shapes which had a typical morphology prepared by water atomization process. Fig. 3 showed the XRD diffractography of the as-atomized powder of BS40 and BS40-A. It can be observed that the raw powders showing predominantly β phase peak at 43.28°, 62.87° and 79.39°. The analysis result is agreeable with the status that the raw powder were prepared by water atomized rapid solidification method, rapid cooled from the β phase field retains a single β phase in the powders, referring to the Cu–Zn binary phase diagram.

3.2. Mechanical properties

Fig. 4 shows the nominal stress versus nominal strain curve of the extruded alloying and premixed samples with different Ti content. The photograph of the tensile sample employed at present paper is illustrated in the figure. It is found that the content of Ti addition has an observable influence on mechanical properties of brass alloys. The yield strength and ultimate tensile strength show

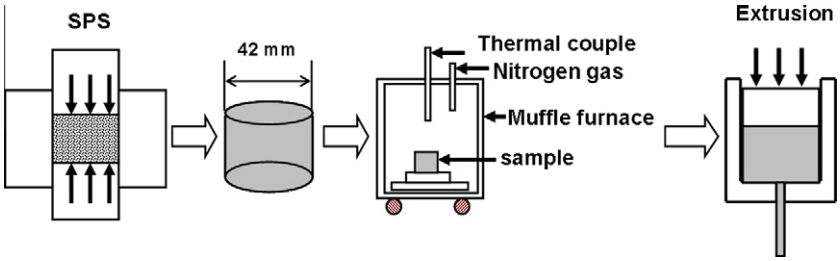

Fig. 1. Schematic sketch of the experimental procedure used to preparing samples.

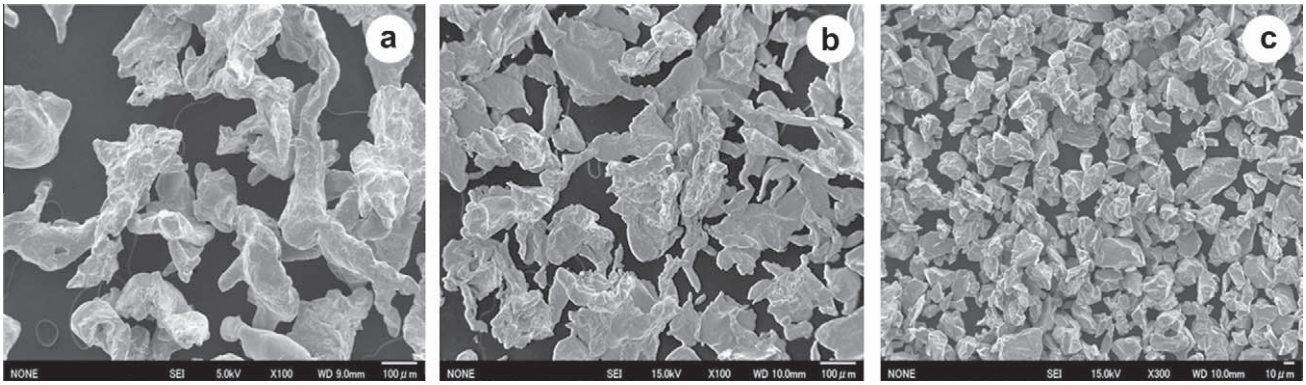

Fig. 2. FE-SEM microstructures of the water atomized alloy powders. (a) BS40; (b) BS40-A; (c) Ti.

Author's personal copy

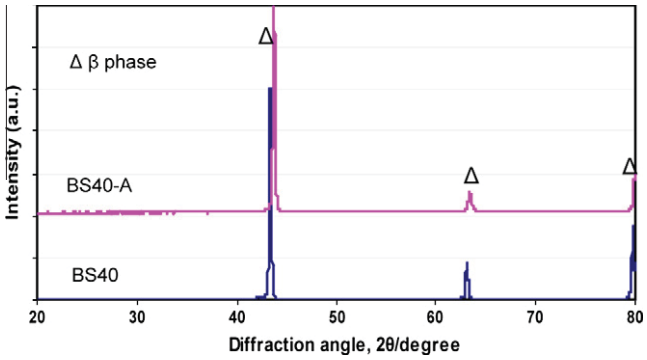

Fig. 3. X-ray diffractography of BS40 and BS40-A raw powders.

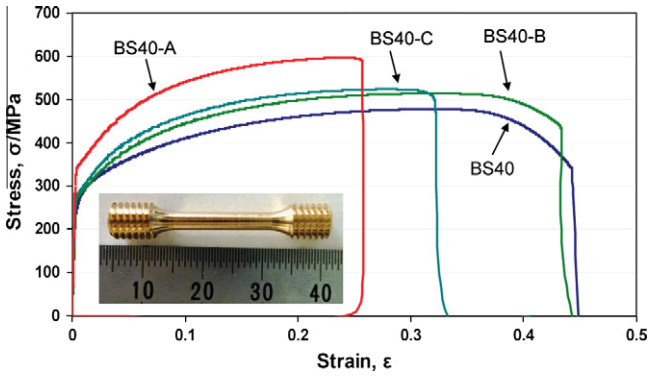

Fig. 4. Nominal stress–nominal strain curves of the extruded alloyed and premixed samples with different Ti content.

an increasing trend with the content of Ti addition increase. BS40-C achieve high yield strength of 290 MPa and tensile strength of 520 MPa, which show 39.4% and 13.5% higher than that of BS40. Unfortunately, the increase of Ti addition shows an deterioration effect on ductility of brass, saying the elongation decrease from 44% to 32.9% when Ti addition increases from 0 wt.% to 1.0 wt.%. The ultimate tensile strength of the extruded BS40-A sample is 597 MPa, 30.4% higher than the extruded BS40, indicating the highest value in all the samples, which is higher than 520 MPa of the extruded premixed BS40-C sample. Furthermore, the yield strength of the extruded BS40-A is 345 MPa, 65.9% higher than the extruded BS40, possessing the highest value which is higher than 290 MPa of the extruded BS40 sample. With respect to the ductility, the extruded BS40 showed highest value of 44.0%, maintained best ductility than the other samples. The extruded BS40-A showed an elongation of 25.2%, lower than that of the extruded BS40-C. Based on the results as aforementioned, Ti addition with different processing methods, saying of premixing or alloying, showed significant effects on mechanical properties of BS40 alloy.

3.3. X-ray diffraction analysis

The X-ray diffractography of the extruded BS40, BS40-A and BS40-C samples prepared by SPS are shown in Fig. 5. It can be observed that peaks appeared at 42.32°, 49.27° and 72.24° besides β phase peaks, which are α phase peaks, suggesting phase transformation of β to α + β duplex phases structure after the raw powder experiencing thermal histories such as sintering at 1073 K, preheating at 923 K and extrusion at 673 K, and pressing deformation. In addition, the minor peak is detected at 42.54° by narrow scan method, which is considered to be the main peak of TiO. Furthermore, the others phases conceivable presenting in reaction between Ti and CuZn were hard to be detected, because of the very low amount of these phases in samples, the phases should be confirmed by qualitative morphological characterization by SEM/EDS analysis.

3.4. Microstructure

Fig. 6 shows of the longitudinal and transverse cross-section of the extruded samples. The longitudinal cross-section shown in Fig. 6a is extruded BS40 sample, indicating the morphology of indiscrete coarse α-phase grain elongated along the extrusion direction in β-phase matrix. The phase structure consists of α-phase crystals precipitated in β-phase matrix, due to the nucleation of α-phase grains during cooling after sintered at 1073 K, and subsequently hot extruded at 928 K. The raw powder of BS40 and BS40–1.0Ti are completely constituted by β-phase (as shown in Fig. 3) before sintering and hot extrusion. The α + β duplex phase structure came into being by phase transformation of the parent β-phase at high temperature of sintering and subsequently extrusion. The extrusion deformation in hot extrusion also provided energy required during phase transformation from β

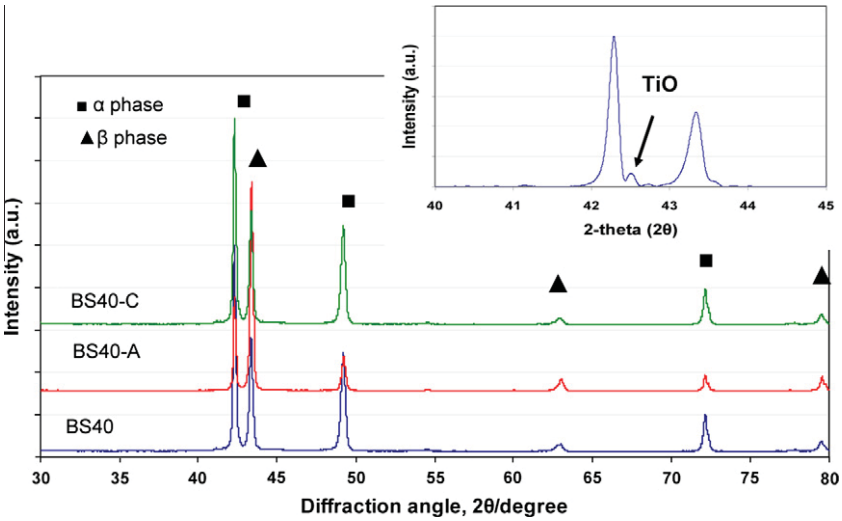

Fig. 5. X-ray diffractography of the extruded alloyed and premixed samples prepared by spark plasma sintering.

Author's personal copy

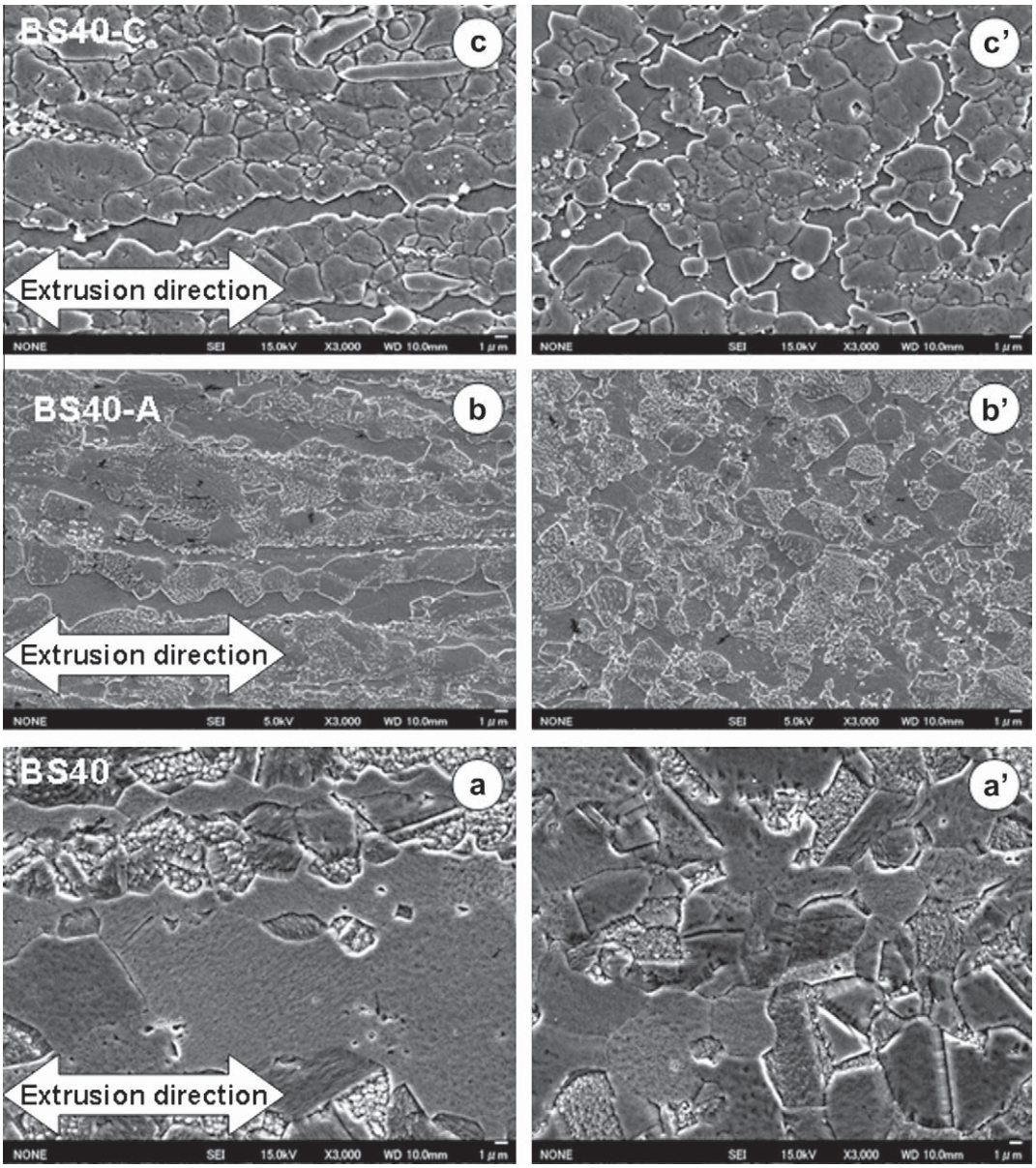

Fig. 6. FE-SEM micrographs of the longitudinal and transversal cross-section of the extruded samples. (a–a′) BS40, (b–b′) BS40-A and (c–c′) BS40-C.

phase to α + β duplex phase structure. The average equivalent diameter of α-phase grain size is approximately 6 μm in the transversal cross-section as shown in Fig. 6a′.

The morphological features of the extruded BS40-A compact are shown in Fig. 6b, b′, which show quite different microstructures when compared with the BS40 sample. The continuous α-phase grains are finer and elongated along the extrusion direction in β-phase matrix, comparing with the microstructures of extruded BS40 shown in Fig. 6a, a′, which indicates Ti is a beneficial element for grain refinement. The maximum solubility of Ti in copper is 8 at.% at 1158 K, while at room temperature the solubility is <1.0 at.% [12]. The maximum solubility of Ti in Zn is 0.027 at.% at room temperature [13]. These data implies the solid solubility of Ti in Cu40Zn alloy less than that of Ti in copper, higher concentration of Ti leads to precipitation.

The EDS analysis at present study exhibits the solubility of Ti is 1.13 at.% in as-atomized raw powder of BS40-A. After sintered and extruded, the solubility of Ti decrease to 0.20 at.% in β-phase, and 0.20 at.% in α-phase. Remained Ti precipitates in form of ultrafine Cu_2TiZn intermetallic compound (IMC), distributing uniformly in the matrix [14], it is not possible to detect the chemical compositions of the IMC because of the small size and quantity of that phase. Furthermore, EDS analysis result also indicates a concentration of 0.67 at.% O in the raw BS40-A alloy powder. Fine particle can be detected at point 2 and point 4 in Fig. 7a, which is considered to be the particles of TiO, the result is consistent with the XRD analysis as shown in Fig. 5. Portion of the oxygen is originated in the preparation of the raw powder by water atomization process as shown in Table 1. Further oxidation resulted from the sintering during SPS and preheating before extrusion (see Table 2). The TiO particles are inferior in bonding with matrix (as shown in Fig. 7a and Table 3), which deteriorates the ductility of BS40-A, saying 25.2%, which is lower than that of extruded BS40 and BS40-C.

The extruded BS40-C sample shows quite different microstructural and morphological characteristics (see Fig. 6c, c′), compared with that of the extruded BS40 and BS40-A. The α-phase primary grains elongated along the extrusion direction in β-phase matrix, plentiful of ultrafine Cu_2ZnTi intermetallic compound (IMC) and

Author's personal copy

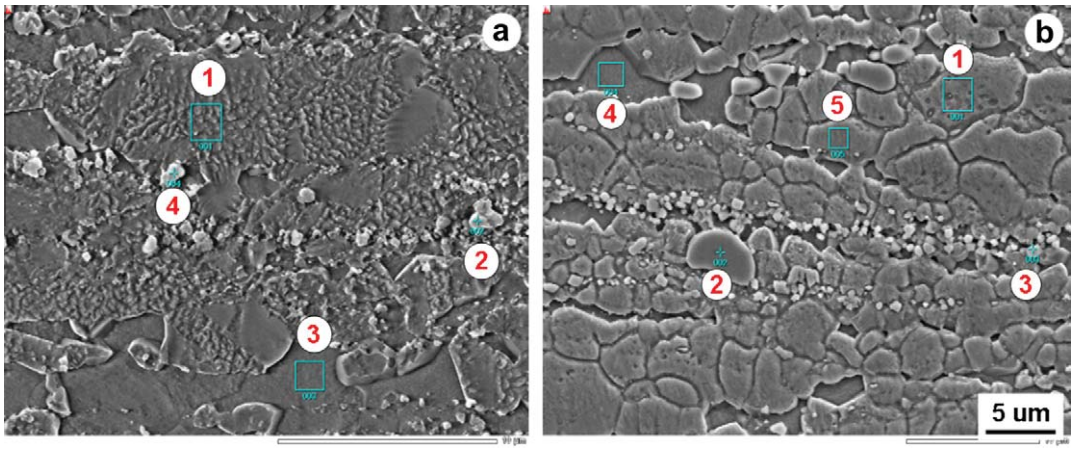

Fig. 7. EDS analysis of the extruded samples. (a) BS40-A and (b) BS40-C.

Table 2
The tensile test results of the extruded alloyed and premixed samples with different Ti contents.

Materials	0.2%YS (MPa)	UTS (MPa)	Elongation (%)
BS40	208	458	44
BS40-B	278.3	514.8	38.3
BS40-C	290.1	520.3	32.9
BS40-A	345.5	597.1	25.2

CuZnTi metastable phase particles can be observed dispersed in α-phase secondary grain boundaries (see Fig. 7b and Table 3), which suggest the dispersoids of Cu_2ZnTi and CuZnTi particles redound to grain refinement during the α-phase recrystallization. In additional, the EDS analysis shows that the α-phase has higher solubility of 0.38 at.% for Ti than the β-phase of 0.08 at.% in premixed BS40-B.

4. Discussion

The extruded samples prepared for this work, using BS40 alloy powder and BS40-A alloy powder as raw materials. BS40 and BS40-A alloy powders were prepared by water atomized method with high cooling rate. To understand the effects of Ti contents on properties of brass, the powders of BS40-B and BS40-C were prepared by premixing BS40 powder and Ti powder.

The results suggest that the content of Ti addition has an observable influence on mechanical properties of brass. The yield strength and ultimate strength show an increasing trend with the content of Ti addition increase. On the other hand, Ti addition shows adverse influence on ductility of brass, accordingly, the content of Ti addition should be elaborately weighted combining with the yield strength and ultimate strength.

A high cooling rate can lead to the formation of a more refined microstructure and extended solid solubility and even metastable phases [15,16]. Rapid cooling rate retained single β phase in the powders, and super-saturated solid solubility of 1.13 at.% Ti in BS40-A powder are formed. The solid solubility of Ti in brass decreases rapidly after experiencing different thermal histories, the equilibrium solubility of Ti in brass are 0.2 at.% in both α phase and β phase. The ternary phase diagram shows that the β phase has higher solubility for Ti than the α phase at equilibrium conditions [17]. However, at the non-equilibrium conditions, the solid solubility of Ti in α phase and β phase show different variation trend at present study.

The difference in atomic radius between Ti, Cu and Zn provides a strain field, which is beneficial to the solid solution strength. It is found that Ti has higher solid solution in extruded BS40-A matrix than that of extruded BS40-C (as shown in Table 3), which is beneficial to the solid solution strength of extruded BS40-A. Furthermore, super-saturated Ti in the brass matrix creates a high chemical potential for precipitation reaction of Ti. The ultrafine dispersoids of Cu_2ZnTi precipitated during sintering and consequent extrusion, served as precipitation hardening which increase resistance to grain boundary slip, achieving yield strength of 597 MPa and tensile strength of 345 MPa, which are higher than those of BS40 and BS40-C.

In respect of the extruded BS40-C, which was prepared by premixing BS40 powder and Ti powder, showed different microstructures and mechanical properties although conceiving the same nominal composition as that of BS40-A. Cu_2ZnTi dispersoids and CuZnTi metastable particles are distributed in the grain boundaries, attributing to the reaction between Ti and Cu40Zn at high temperature, and acting as grain refiners, enhancing the mechanical properties. Furthermore, the diffusion between Ti and Cu40Zn at high temperature results in the equilibrium solubility of Ti is

Table 3
Chemical compositions (at.%) of the phase present in the extruded samples detected by SEM/EDS analysis.

Alloy	Phase	% Cu	% Zn	% Ti	% O
(a) BS40-A	1 (α phase)	65.09 ± 2.95	34.71 ± 4.16	0.20 ± 0.55	–
	2 (TiO)	6.80 ± 3.24	5.92 ± 4.56	43.51 ± 0.57	43.77 ± 0.69
	3 (β phase)	56.30 ± 2.63	43.01 ± 3.72	0.20 ± 0.59	0.5 ± 0.18
	4 (TiO)	17.58 ± 2.53	17.06 ± 3.57	41.39 ± 0.46	23.98 ± 0.41
(b) BS40-C	1 (α phase)	64.46 ± 2.46	35.16 ± 3.48	0.38 ± 0.46	0.35 ± 0.23
	2 (Cu_2TiZn)	49.23 ± 1.72	25.25 ± 2.42	25.51 ± 0.32	–
	3 (CuZnTi)	30.55 ± 1.90	31.19 ± 2.68	38.26 ± 0.35	–
	4 (β phase)	57.26 ± 2.50	42.65 ± 3.54	0.08 ± 0.47	–

Author's personal copy

0.38 at.% in α phase and 0.08 at.% in β phase, suggesting the α phase has higher solubility for Ti than the β phase in premixed samples. Precipitations presence in Cu–Ti binary phase system, such as Cu_4Ti (β′), was difficult to be confirmed because of the very low amount of this phase in both extruded alloyed and premixed samples used in the present study.

5. Conclusions

This paper reports on the effects of Ti addition on microstructures and mechanical properties of Cu40Zn brass. Ti additive showed significant precipitation hardening response on mechanical properties of Cu40Zn brass, which could improve the yield strength and ultimate tensile strength distinctly to about 65.9% and 30.4% higher than BS40, respectively. The results suggest the effect of Ti addition on Cu40Zn brass was worthy of further investigation.

Acknowledgements

This work was financially supported by Regional Research and Development Resources Utilization Program, Japan Science and Technology Agency (JST). The authors extend their thanks to Nihon atomized metal powders corporation (Project Manager: Mr. Koji Yamamoto, Mr. Motoi Takahashi and Mr. Eisuke Yotsuka), for providing powders used in this study. And also grateful to San-Etsu metals Co. Ltd., (Project Manager: Mr. Yoshiharu Kosaka and Mr. Akimichi Kojima), for their technical supports in this study. The authors sincerely thank the researchers of the Joining and Welding Research Institute (JWRI) in Osaka University, Mr. Yoshinori Muraki, Ms. Sachiyo Nakamura and Mr. Kyugo Inui for assistant carrying out extrusion experiment.

References

[1] Davis JR. Alloying, understanding the basics. Materials Park OH 44073-0002: ASM International; 2002. p. 364.
[2] Li S, Imai H, Atsumi H, Kondoh K. Characteristics of high strength extruded BS40CrFeSn alloy prepared by spark plasma sintering and hot pressing. J Alloys Compd 2010;493:128–33.
[3] La Fontaine A, Keast VJ. Compositional distributions in classical and lead-free brasses. Mater Charact 2006;57:424–9.
[4] Xiao L, Shu X, Yi D, Zhang X, Qin J, Hu J. Microstructure and properties of unleaded free-cutting brass containing stibium. Trans Nonferr Metal Soc China 2007;17:s1055–9.
[5] Vilarinho C, Davim JP, Soares D, Castro F, Barbosa J. Influence of the mechanical composition on the machinability of brasses. J Mater Process Technol 2005;170:441–7.
[6] Metals handbook, alloy phase diagrams, ASM handbook, vol. 3, 10th ed.; 1990.
[7] Laughlin DE, Cahn JW. Spinodal decomposition in age hardening copper–titanium alloys. Acta Metall 1975;23:329–39.
[8] Poter A, Thompson AW. On the mechanism of precipitation strengthening in Cu–Ti alloys. Scripta Metall 1984;18:1185–8.
[9] Nagarjuna S, balasubramanian K, Sarma DS. Effect of prior cold work on mechanical properties, electrical conductivity and microstructure of aged Cu–Ti alloys. J Mater Sci 1999;34:2929–42.
[10] Kumar KCH, Ansara I, Wollants P, Deliaaey L. Thermodynamic optimization of the Cu–Ti system. Z Metall 1996;87:666–72.
[11] Imai H, Kosaka Y, Kojima A, Li S, Kondoh K. Characteristics and machinability of lead-free P/M Cu60–Zn40 brass alloys dispersed with graphite. Powder Technol 2010;198:417–21.
[12] Binary alloy phase diagrams, Metals handbook, vol. 1, Metals Park, OH, ASM; 1986. p. 820.
[13] Murray JL. Phase diagram of binary titanium alloys. ASM Int.; 1987.
[14] Heine W, Zwecker U. Phases of B2-structure type (CsCl-type) in ternary systems with copper and nickel (in German). Naturewissenschaften 1962;17:391–5.
[15] Jones H. Cooling rates during rapid solidification from a chill surface. Mater Lett 1996;26:133–6.
[16] Katgerman L, Dom F. Rapid solidified aluminum alloys by melt spinning. Mater Sci Eng A 2004;375–377:1212–6.
[17] Soares D, Vilarinho C, Castro F. Contribution to the knowledge of the Cu–Zn–Ti system for compositions close to brass alloys. Scand J Metall 2001;30:254–7.